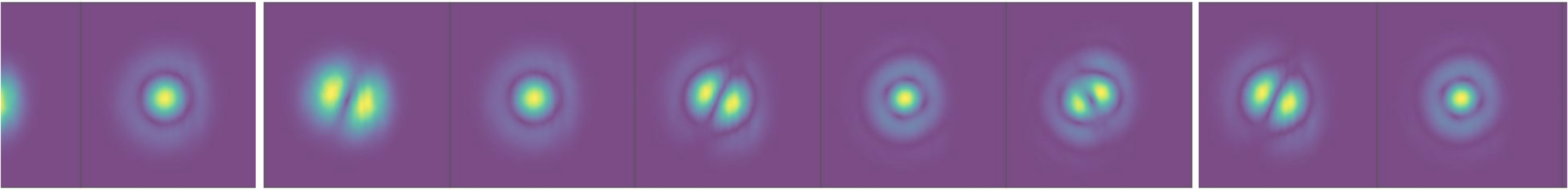

Locked cavity scan
using heterodyne detection with a phase camera

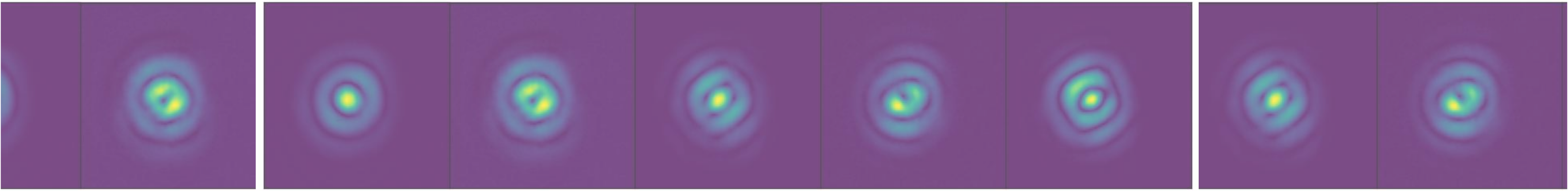

Ricardo Cabrita

Aaron Goodwin-Jones, Joris van Heijningen, Pavel Demin, Martin van Beuzekom, Matteo Tacca, Giacomo Bruno, Clement Lauzin

Bologna, ET Symposium 28 May 2025

ricardo.cabrita@uclouvain.be

Increasing circulating power in GW detectors

Next generation detectors

Arm circ. power	CE	ET (HF)
	1.5 MW	3 MW

Increasing circulating power in GW detectors

Next generation detectors

Arm circ. power	**CE**	**ET (HF)**
	1.5 MW	3 MW

Current detectors

Arm circ. power	**LIGO A+**	**AdV +**
design	750 kW	150 kW
actual	**350 kW**	**96 kW**

Increasing circulating power in GW detectors

Next generation detectors

Arm circ. power	CE	ET (HF)
	1.5 MW	3 MW

Current detectors

Arm circ. power	LIGO A+	AdV +
design	750 kW	150 kW
actual	**350 kW**	**96 kW**

Power losses to

- scattering,
- point defects,
- ITF working point degradation – over 6 hour thermal transient in LIGO.

(some) issues with high optical power

Thermal effects can shift the cavity eigenmodes

Simulation by J. Degallaix – Virgo report VIR-0831A-24

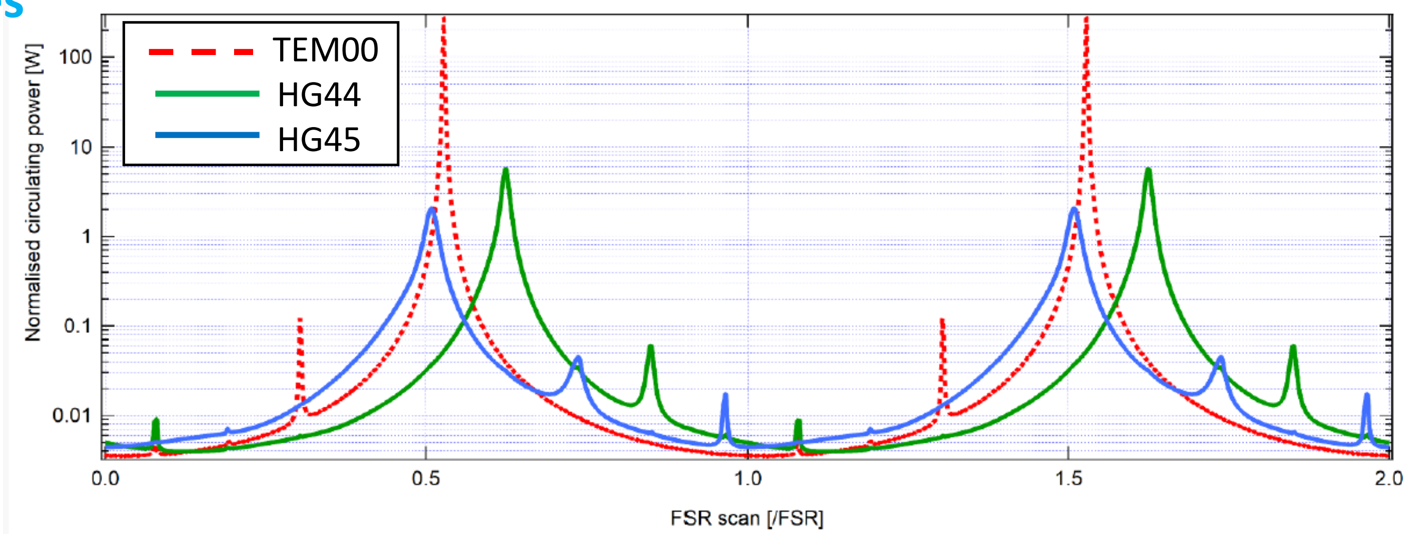

(some) issues with high optical power

Thermal effects can shift the cavity eigenmodes

Simulation by J. Degallaix – Virgo report VIR-0831A-24

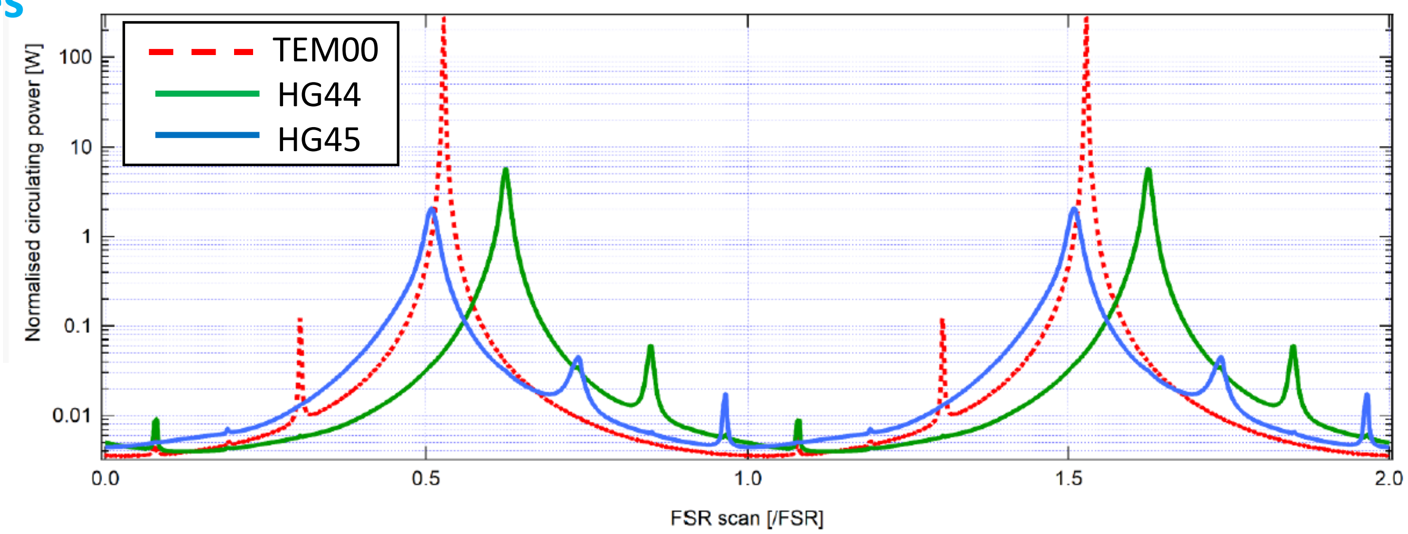

Parametric instabilities

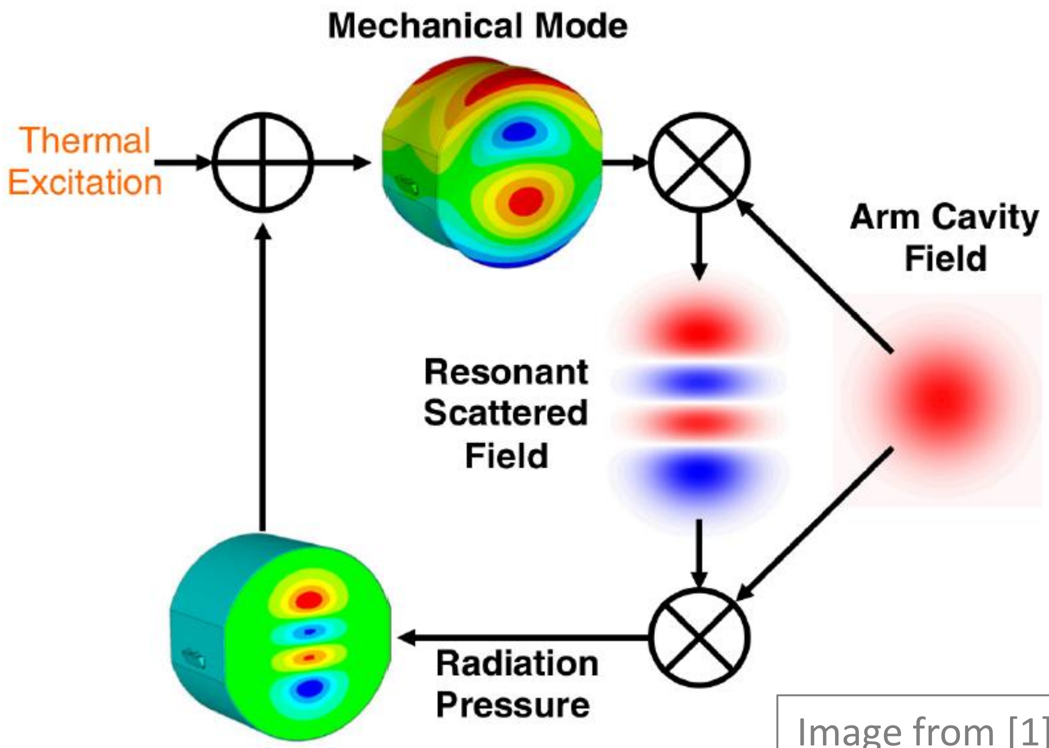

Image from [1]

high power + optical HOM overlapping with acoustic mode + radiation pressure

Suppression by injecting HOM with opposing phase (V. Bossilkov) [2]

Cavities with high circulating power…

With continuous wave laser….

$$I = {}^{2P}/_{\pi w_0^2}$$

Group	Tot. Pwr. (MW)	Intensity (MW/cm^2)	Waist (mm)	Application
H. Mueller:	0.14	123000	0.0085	PEM/dipole trapping
LIDA	0.124	4700	0.0285	Dark matter detection
LIGO	0.350	0.154	12	GW detection
IJClab (ps laser)	0.710	0.56	9	Extreme radiation/accelerators
Photodetachment	10	636	1	Fusion reactor – neutral beam
ET (CE)	3	0.95	14.2	GW detection

Cavities with high circulating power…

With continuous wave laser….

$$I = {}^{2P}/_{\pi w_0^2}$$

Group	Tot. Pwr. (MW)	Intensity (MW/cm^2)	Waist (mm)	Application
H. Mueller:	0.14	123000	0.0085	PEM/dipole trapping
LIDA	0.124	4700	0.0285	Dark matter detection
LIGO	0.350	0.154	12	GW detection
IJClab (ps laser)	0.710	0.56	9	Extreme radiation/accelerators
Photodetachment	10	636	1	Fusion reactor – neutral beam
ET (CE)	3	0.95	14.2	GW detection

unique to GW detection: Combination of high power with very low losses!

Mode sensing and control in Virgo

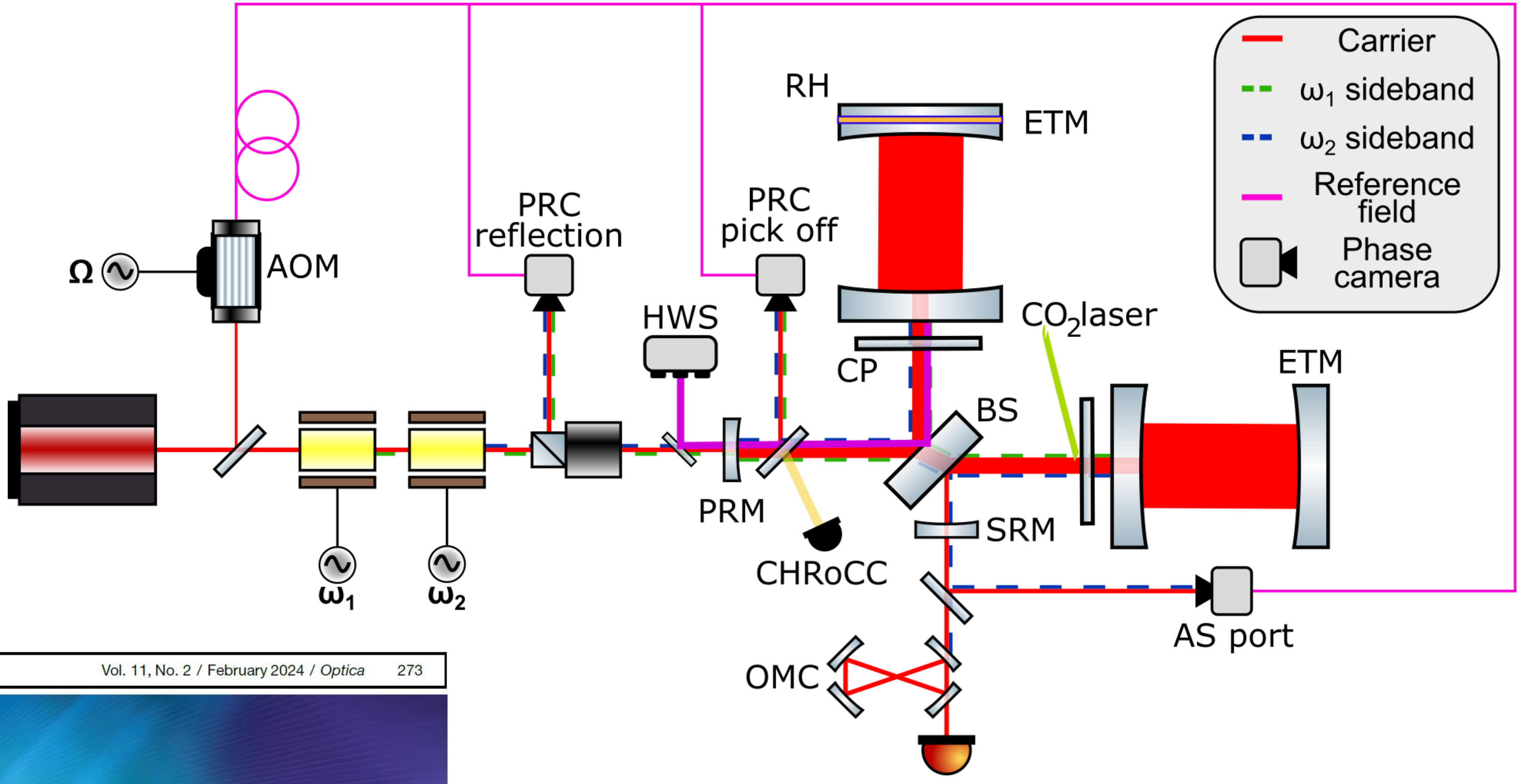

Image adapted from [3]


Review Vol. 11, No. 2 / February 2024 / *Optica* 273

OPTICA

Transverse mode control in quantum enhanced interferometers: a review and recommendations for a new generation

Aaron W. Goodwin-Jones,[1,2,*] Ricardo Cabrita,[3] Mikhail Korobko,[4] Martin Van Beuzekom,[5] Daniel D. Brown,[1,6] Viviana Fafone,[7,8] Joris Van Heijningen,[3] Alessio Rocchi,[8] Mitchell G. Schiworski,[1,6] and Matteo Tacca[5]

- No feedback loop
- No way to online monitor thermal transient.

Locked cavity monitoring with the phase camera

Optical injection scheme + phase camera

- Monitoring cavity g-factor while locked
- Test phase sensitive measurements of HOMs – for PI suppression of HOM of arbitrary order

Locked cavity monitoring with the phase camera

Optical injection scheme + phase camera

- Monitoring cavity g-factor while locked
- Test phase sensitive measurements of HOMs – for PI suppression of HOM of arbitrary order

Table-top set-up at UCLouvain

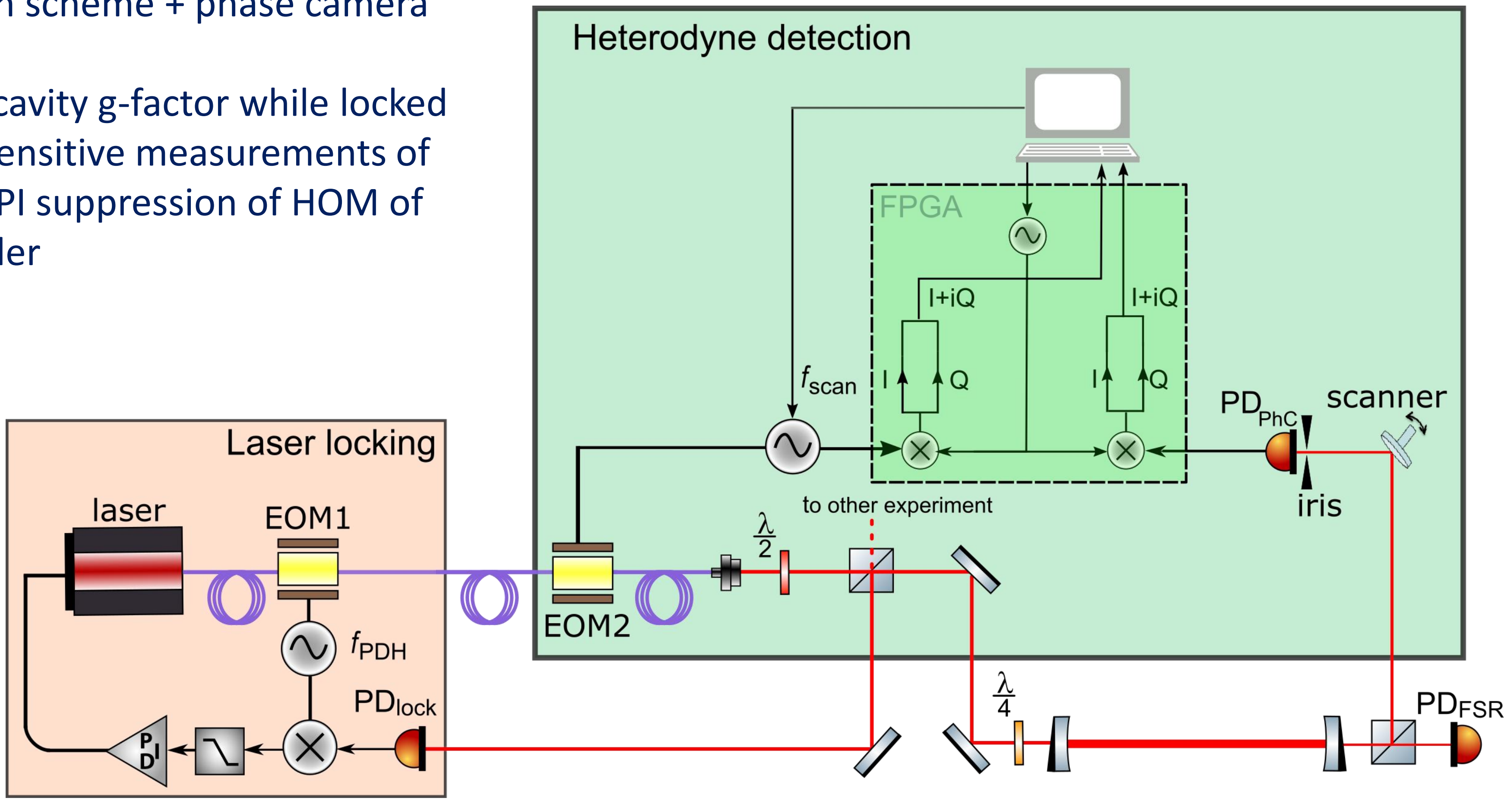

- Invar bar cavity (open air)
- 32 cm, (nominal) Finesse 360

Locked cavity monitoring with the phase camera

Optical injection scheme + phase camera

- Monitoring cavity g-factor while locked
- Test phase sensitive measurements of HOMs – for PI suppression of HOM of arbitrary order

Table-top set-up at UCLouvain

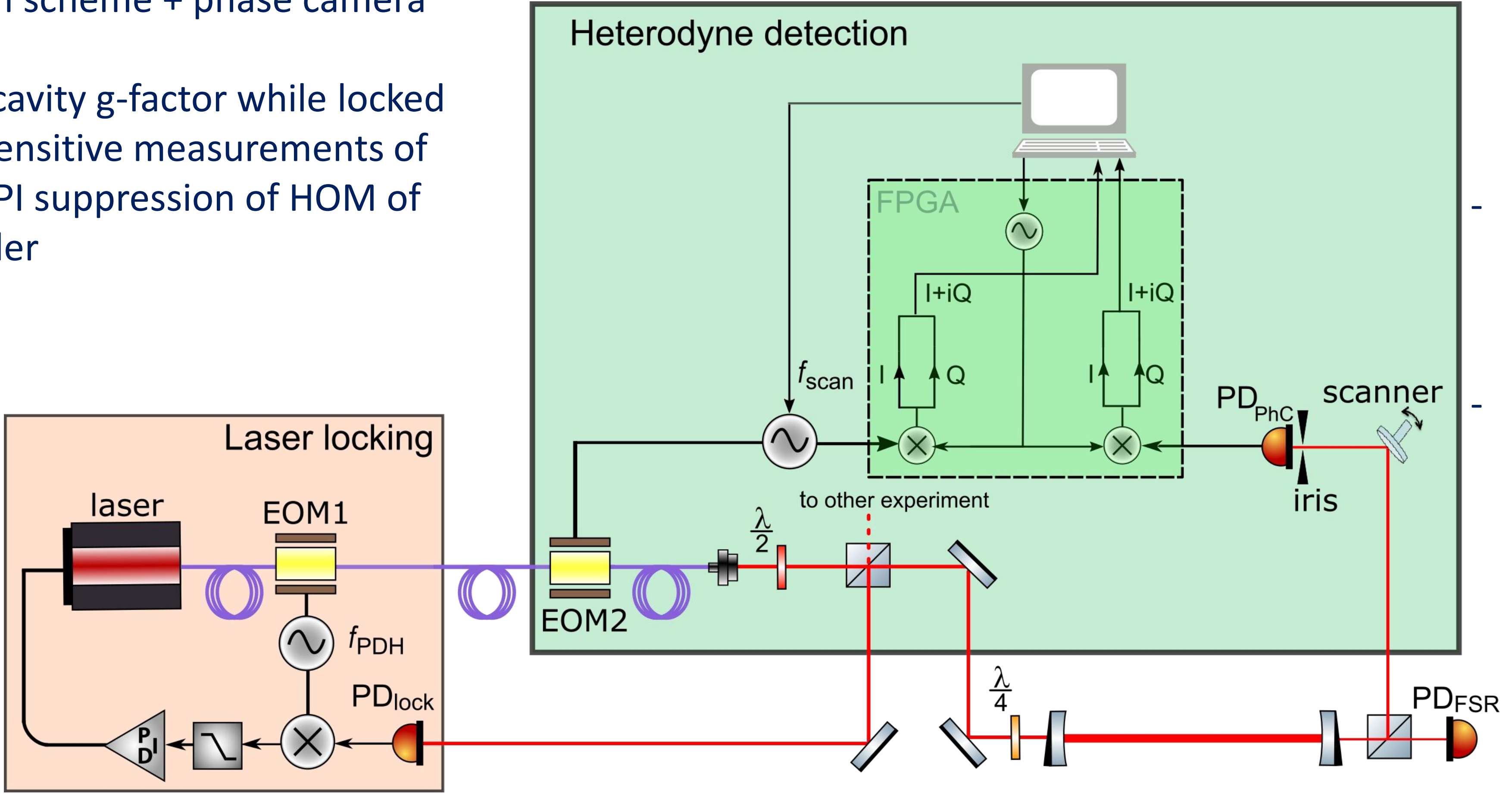

Nikhef

- Custom phase camera similar to Virgo's
- Pinhole photodiode breaks mode orthogonality

- Scanning EOM2 modulation frequency injects sideband HOM at key frequencies

- Invar bar cavity (open air)
- 32 cm, (nominal) Finesse 360

Sideband HOM injection with EOM

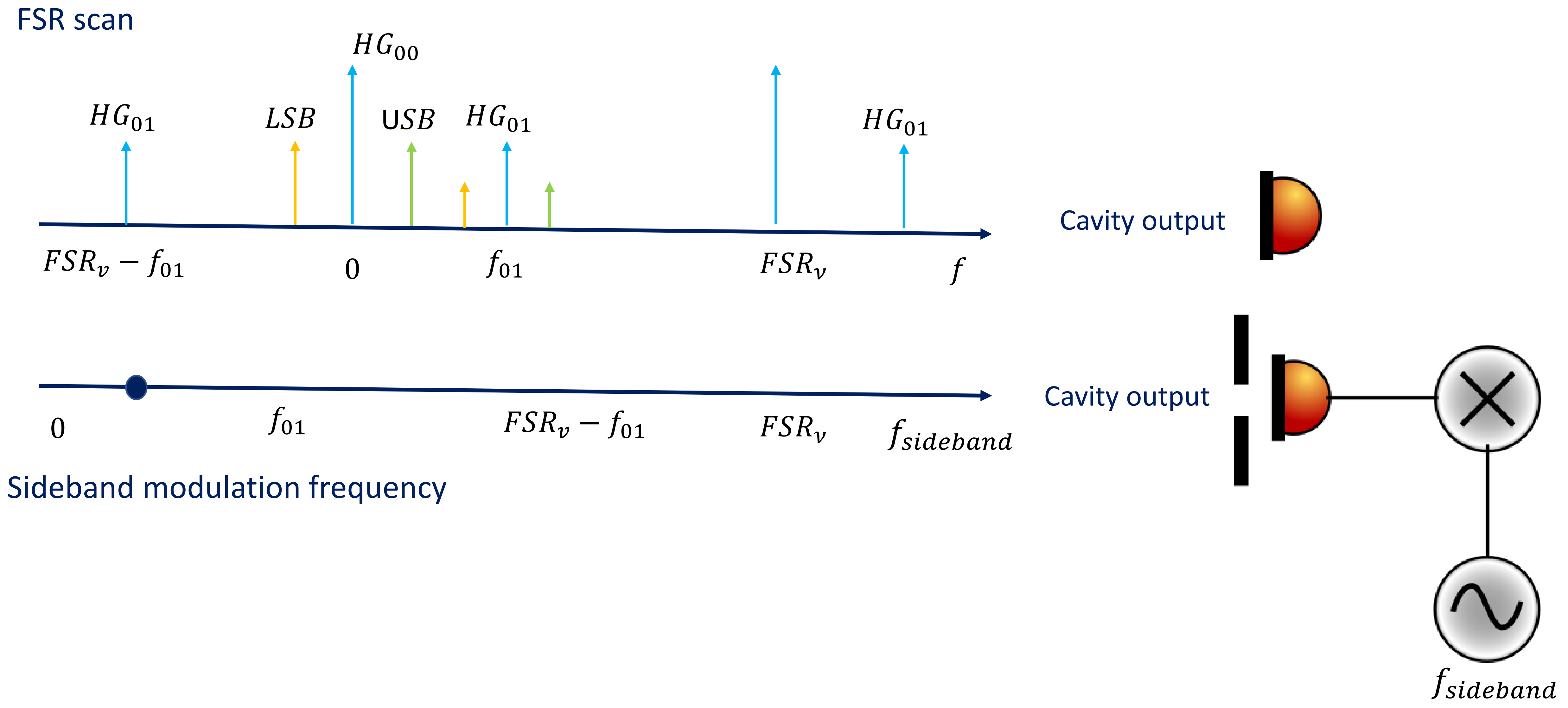

Sideband HOM injection with EOM

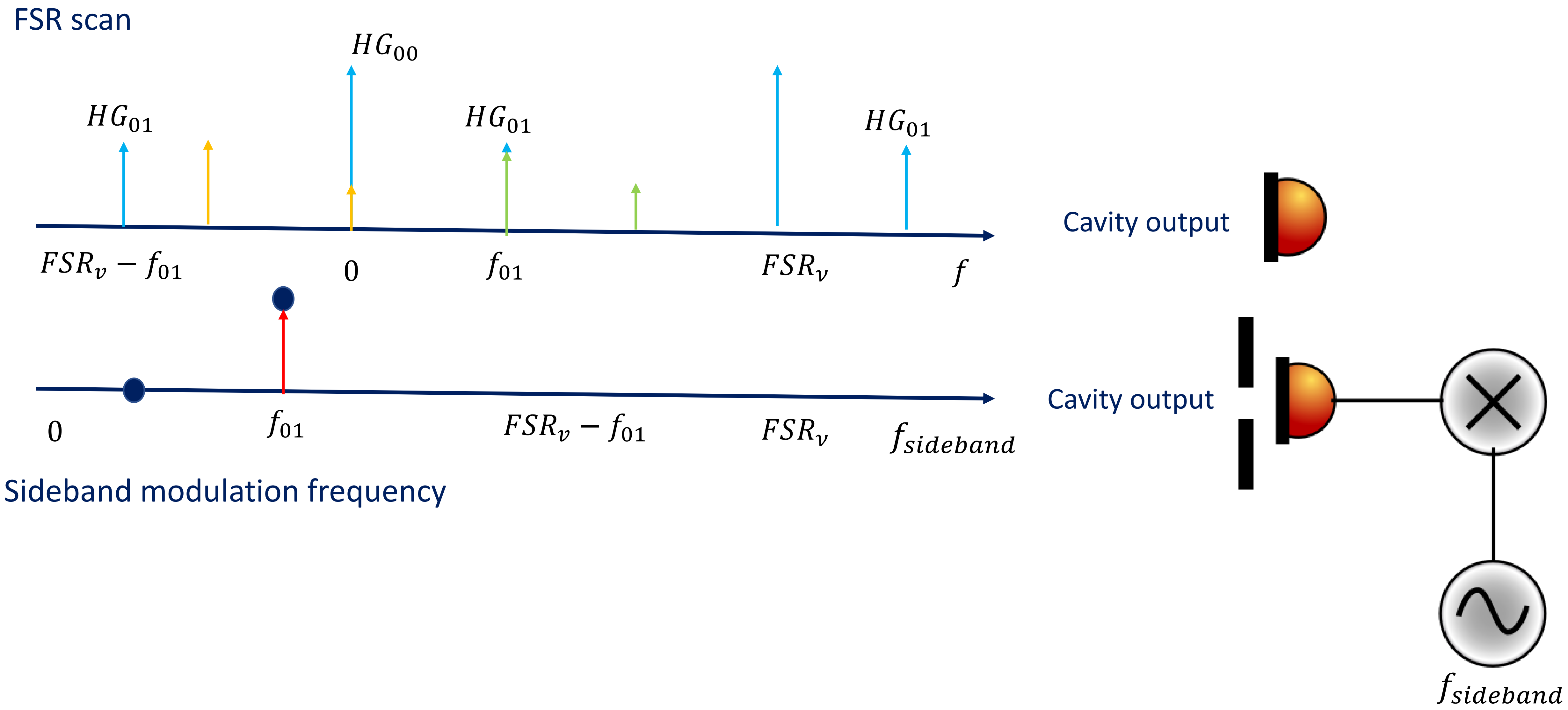

Sideband HOM injection with EOM

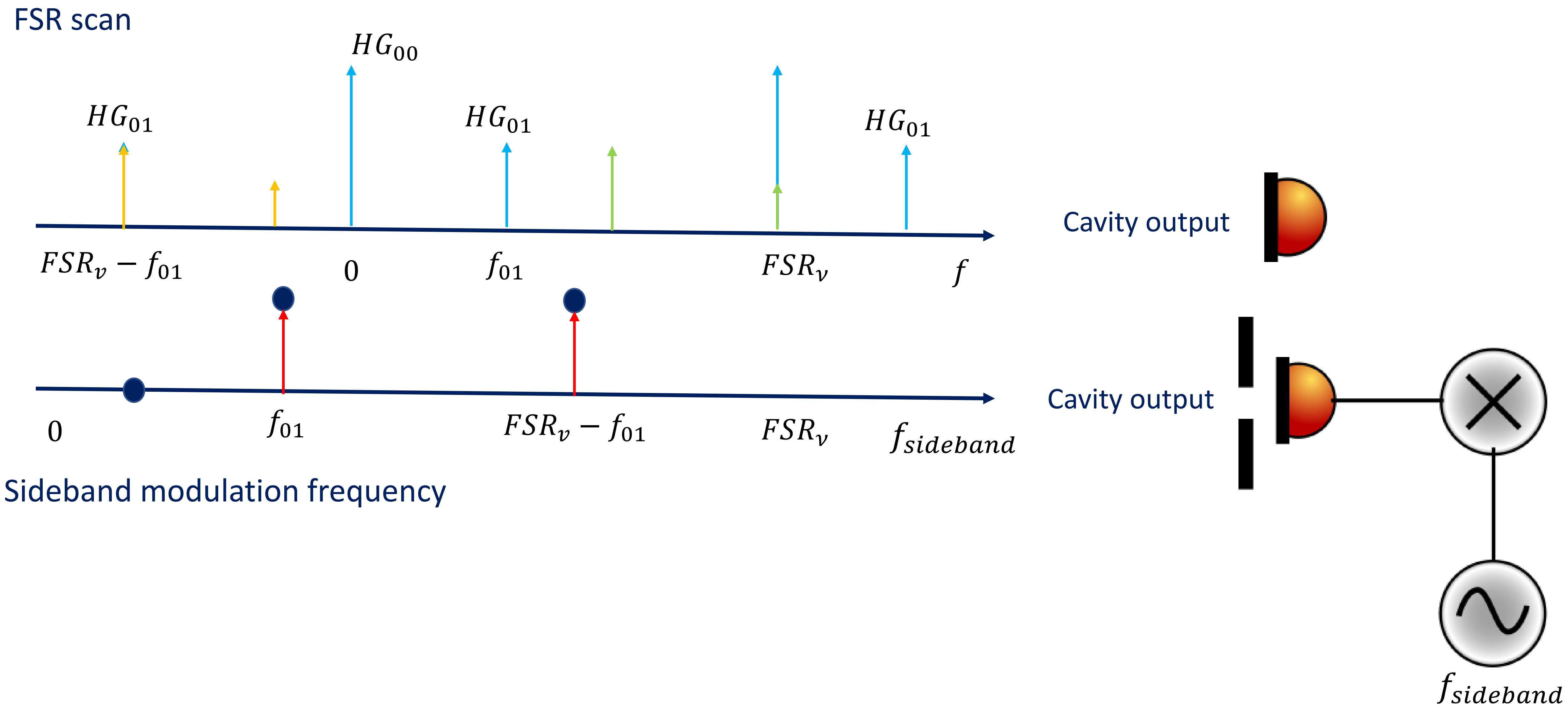

Sideband HOM injection with EOM

We obtain a spectrum from the LSB and another from the USB at $\mathrm{FSR_\nu - f_{m+N}}$!

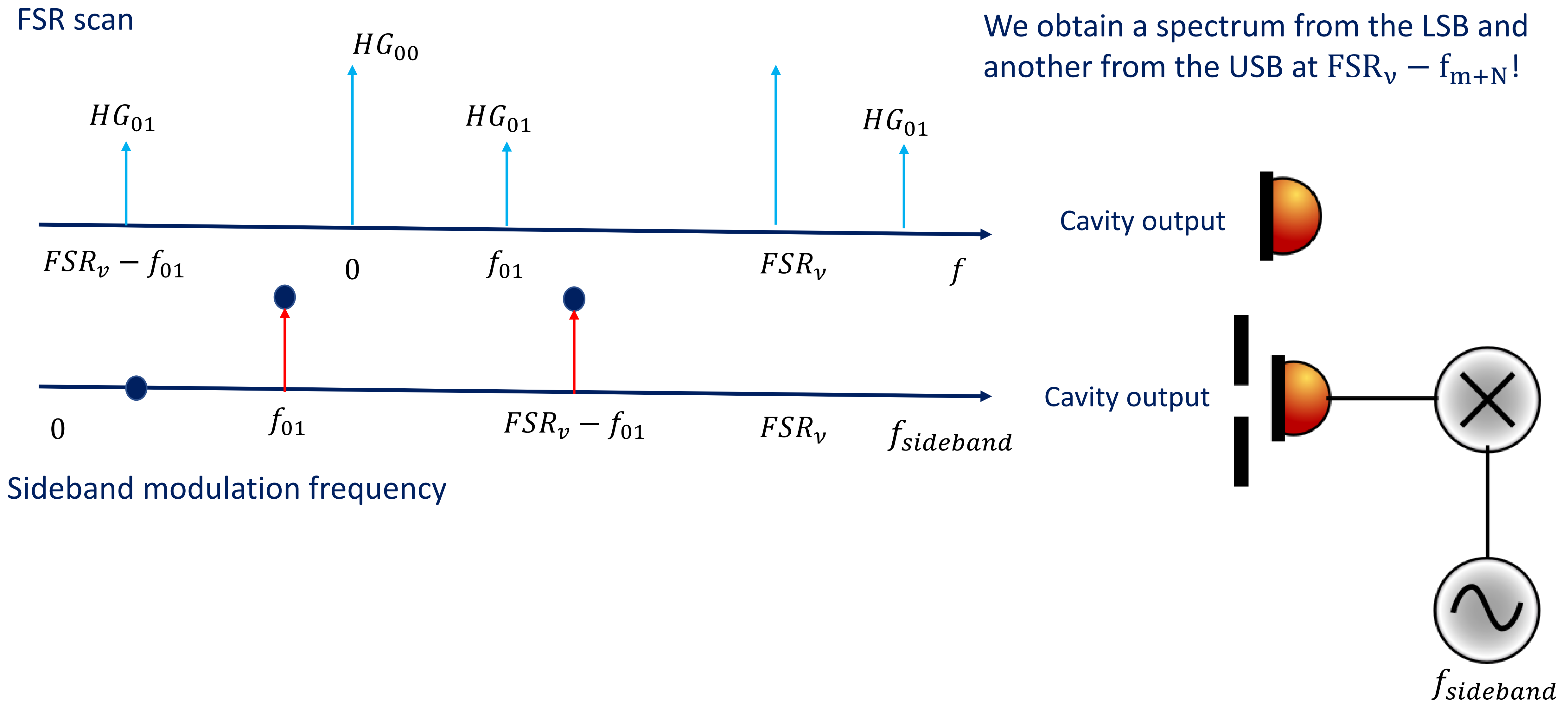

Sideband HOM injection with EOM

FSR scan

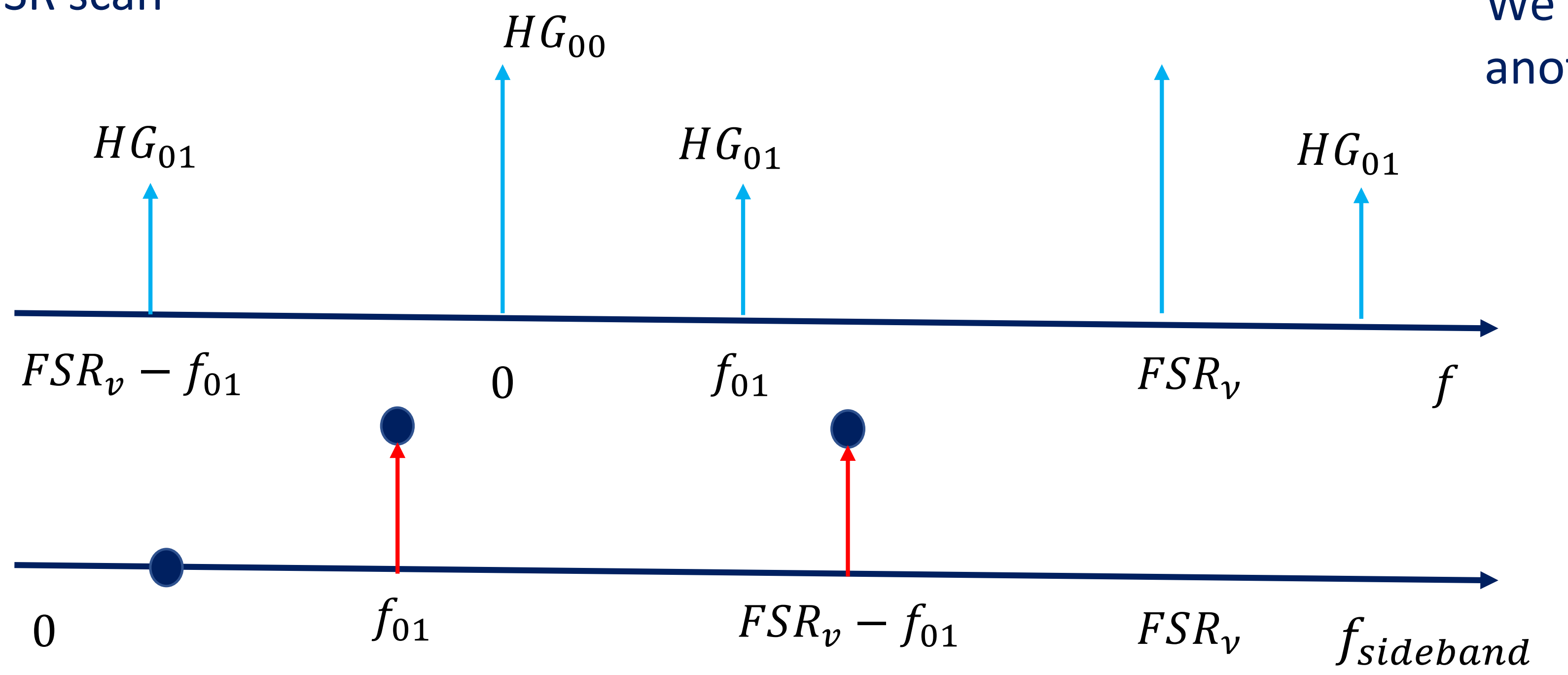

We obtain a spectrum from the LSB and another from the USB at $\mathrm{FSR}_\nu - \mathrm{f}_{m+n}$!

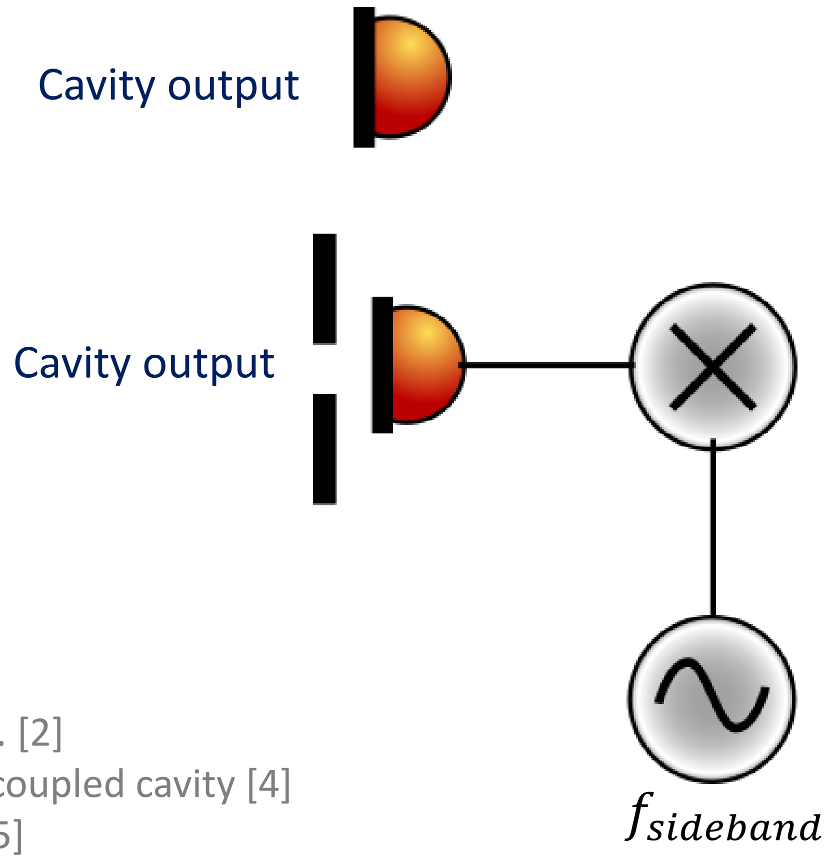

Sideband modulation frequency

Similar sideband injection scheme

- V. Bossilkov – 1st order mode injection + QPD readout – demonstration of PI suppression. [2]
- A. Goodwin Jones – 2nd order mode injection – mode mismatch simulation of linear and coupled cavity [4]
- M. Beaumont and D. Romanini - EOM scan, and blade + photodiode for v-shaped cavity [5]
- O. Schwartz – 1st order mode injection to characterize cavity concentricity (phase-contrast electron microscopy) [6]

Heterodyne scan results

Acquisition limited to 250 MHz but cavity FSR is 467 MHz – LSB probes first half of FSR and USB probes second half of FSR

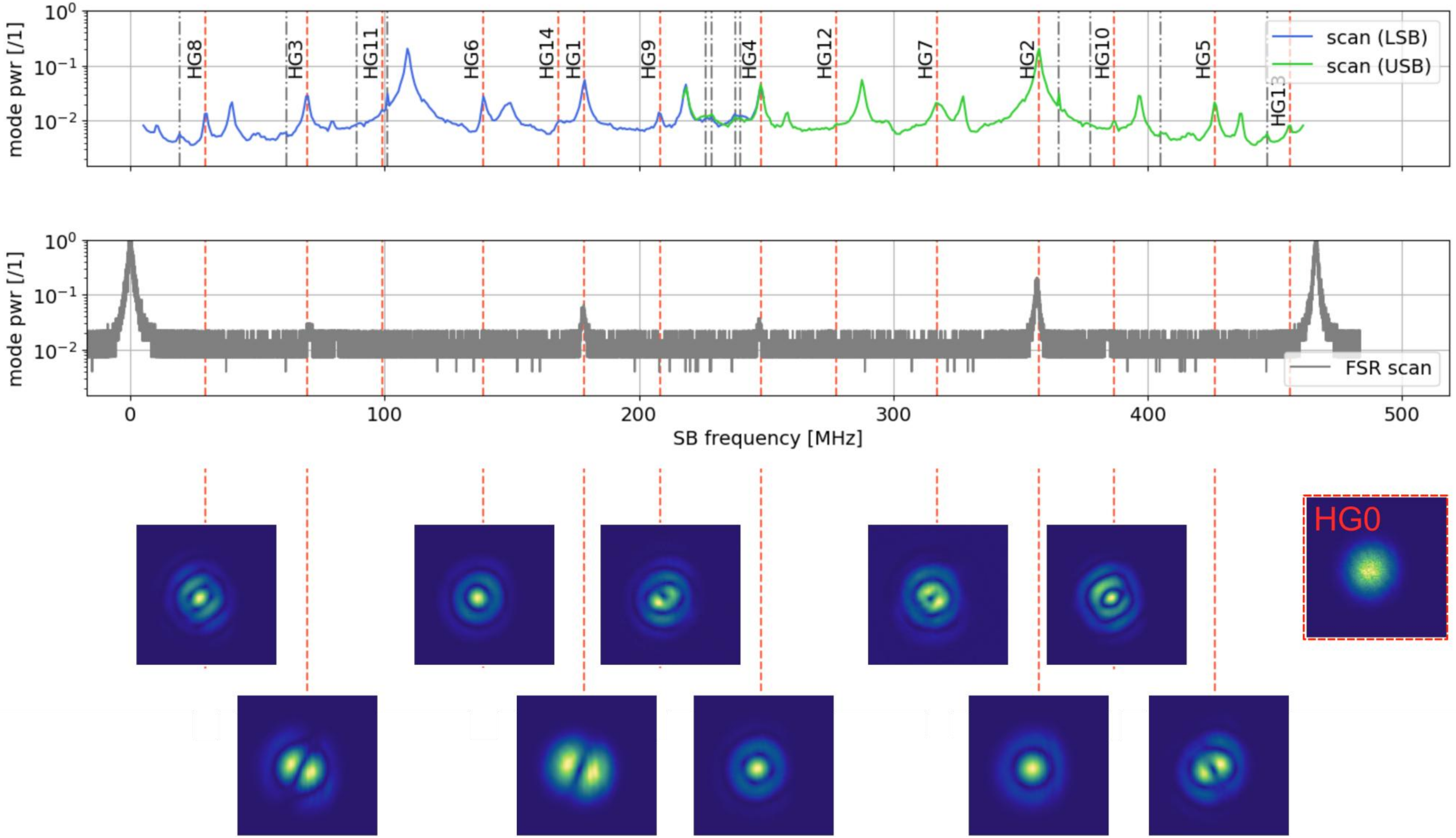

Cavity g-factor measurement while locked

Fit mode positions for LSB:

$$f_{LSB}(m+n) = \mathrm{FSR}_\nu \frac{m+n}{\pi} \arccos(1 - \mathrm{L/RoC})$$

Fit mode positions for USB

$$f_{USB}(m+n) = \mathrm{FSR}_\nu - \mathrm{FSR}_\nu \frac{m+n}{\pi} \arccos(1 - \mathrm{L/RoC})$$

Mode fitting results….

Mirror RoC	0.501992 ± 0.000070 m
Cavity length	0.321518 ± 0.000030 m
Cavity FSR	466.213 ± 0.043 MHz
Cavity g-factor	0.35951 ± 0.00017 MHz

Cavity g-factor measurement while locked

Fit mode positions for LSB:

$$f_{LSB}(m+n) = \mathrm{FSR}_\nu \frac{m+n}{\pi} \arccos(1 - \mathrm{L}/\mathrm{RoC})$$

Fit mode positions for USB

$$f_{USB}(m+n) = \mathrm{FSR}_\nu - \mathrm{FSR}_\nu \frac{m+n}{\pi} \arccos(1 - \mathrm{L}/\mathrm{RoC})$$

Mode fitting results….

Mirror RoC	0.501992 ± 0.000070 m
Cavity length	0.321518 ± 0.000030 m
Cavity FSR	466.213 ± 0.043 MHz
Cavity g-factor	0.35951 ± 0.00017 MHz

Different modes experience different round-trip losses (RTL):
– can be exploited to make RTL map.

	FWHM [MHz]	RTL [%]
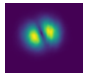	1.75 ± 0.07	0.66
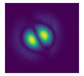	1.83 ± 0.08	0.77
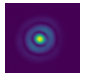	1.57 ± 0.09	0.42
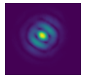	1.68 ± 0.16	0.57
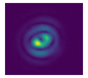	1.74 ± 0.26	0.64
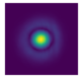	1.74 ± 0.044	0.65
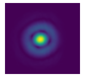	1.76 ± 0.046	0.67
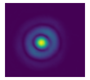	1.70 ± 0.083	0.60

Phase sensitive measurements

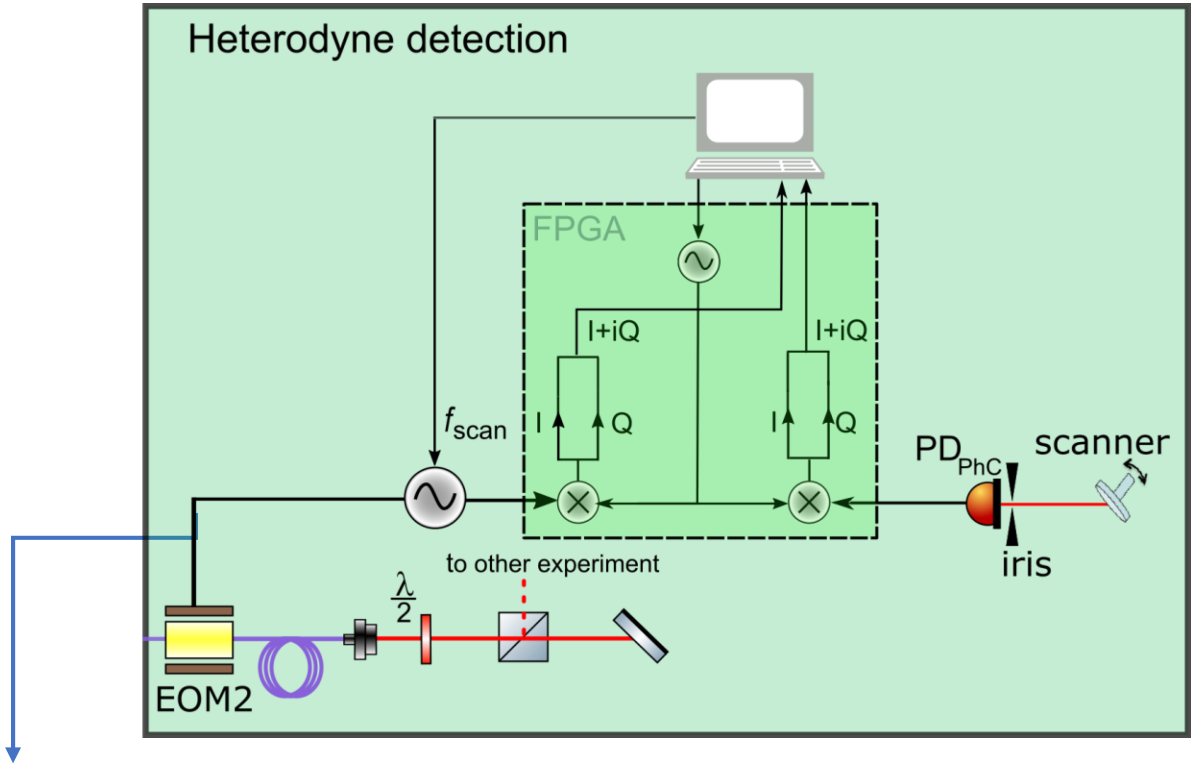

$$\Phi_{beat} = \Delta R - \Delta G + \Delta L + \Delta K + \Delta\phi_{M0}$$

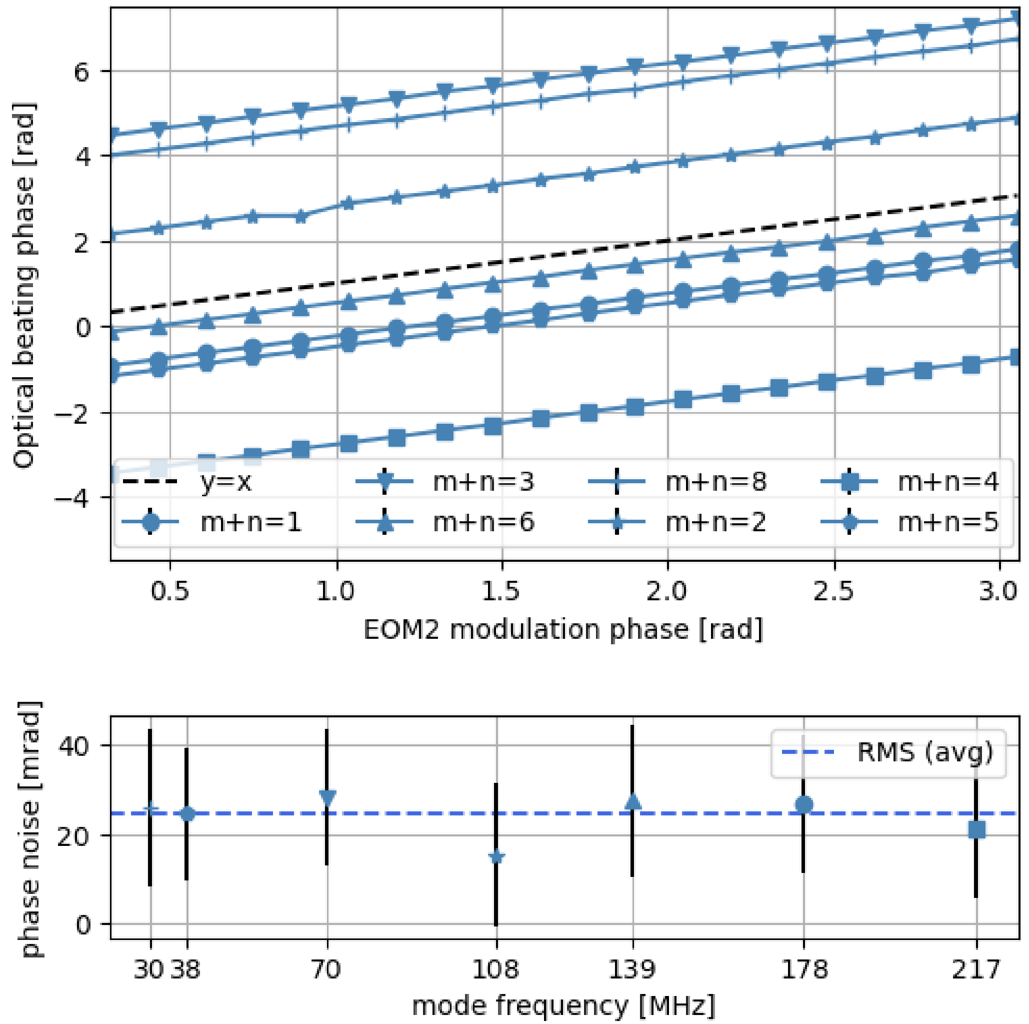

- Phase of EOM2 modulating sine is swept.
- Phase camera retrieves optical beating phase between carrier and sideband HOM – arctan(Q/I)

- Phase camera can be used for PI suppression of arbitrary HOMs
- Can also be used for mode mismatch and misalignment signals in transmission

Towards the MW goal in next generation detectors

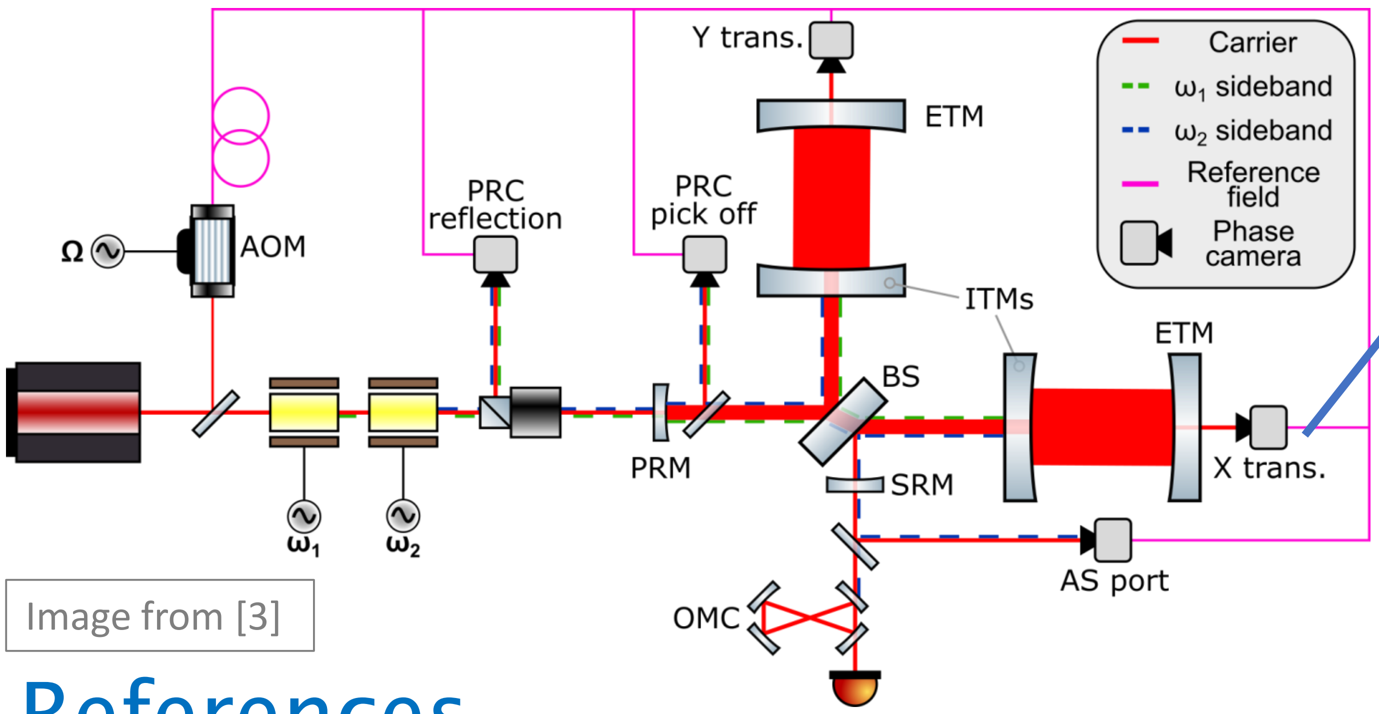

Image from [3]

Preprint available on arXiv:
https://arxiv.org/abs/2505.03525

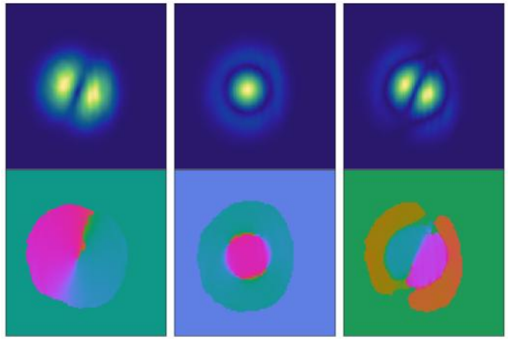

We propose testing the technique at Virgo

ET-OPT @ UCLouvain

Poster by Dr. Aaron Goodwin-Jones

ricardo.cabrita@uclouvain.be

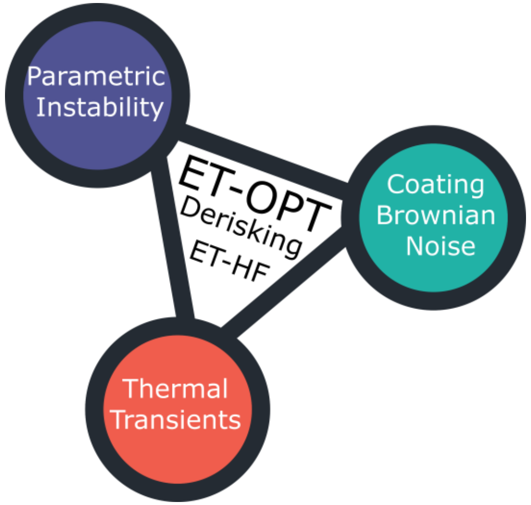

References

[1] M.Evans et al., ‘’ Observation of parametric instability at LIGO’’ Phys. Rev. Lett. 114, 161102 (2015)
[2] V. Bossilkov, Jian Liu et al., ‘’Demonstration of the parametric instability suppression through optical feebdack‘’ Rev. D 109, 102006 (2024)
[3] A. W. Goodwin-Jones, R. Cabrita, et al., "Transverse mode control in quantum enhanced interferometers: a review and recommendations for a new generation," Optica 11, 273-290 (2024)
[4] A. W. Goodwin-Jones, H. Zhu, et al., "Single and coupled cavity mode sensing schemes using a diagnostic field," Opt. Express 31, 35068-35085 (2023)
[5] M. Beaumont, I. Ventrillardet, et al., "Optical cavity spectroscopy using heterodyne detection with optical feedback laser frequency locking," Appl. Opt. 63, 2227-2233 (2024)
[6] O. Schwartz, J. J. Axelrod, S. L. Campbell, et al., “Laser phase plate for transmission electron microscopy,” Nat.methods 16, 1016–1020 (2019)

Extra Slides

Noise and detection limits

Power in sideband HOM in decibels relative to carrier [dBc]:

$$10\log_{10}\left(|k_{mn}|^2 \frac{P_{SB}}{P_{carr}}\right) \quad [\mathrm{dBc}]$$

Coupling to HOM
(comparison with FSR scan)

Given by EOM calibration

Calibrated noise measurements in dBc units

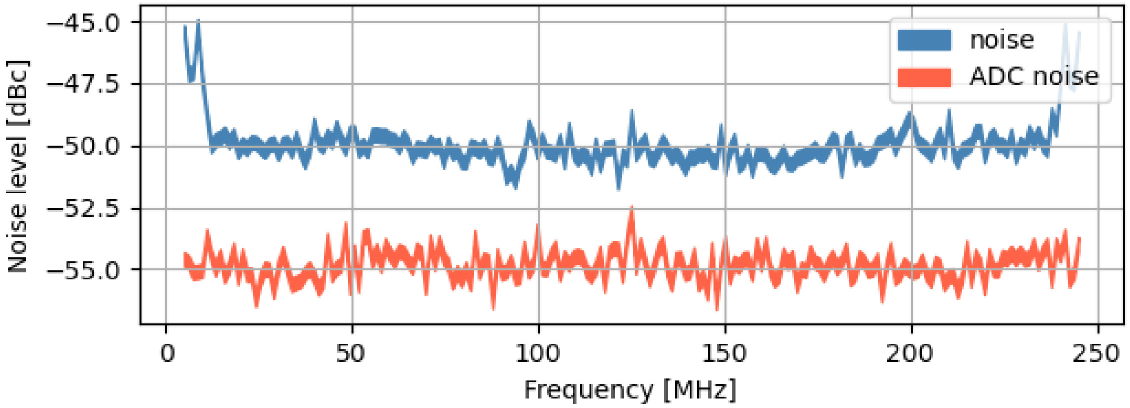

Converted to HOM coupling
assuming 10% sidebands.

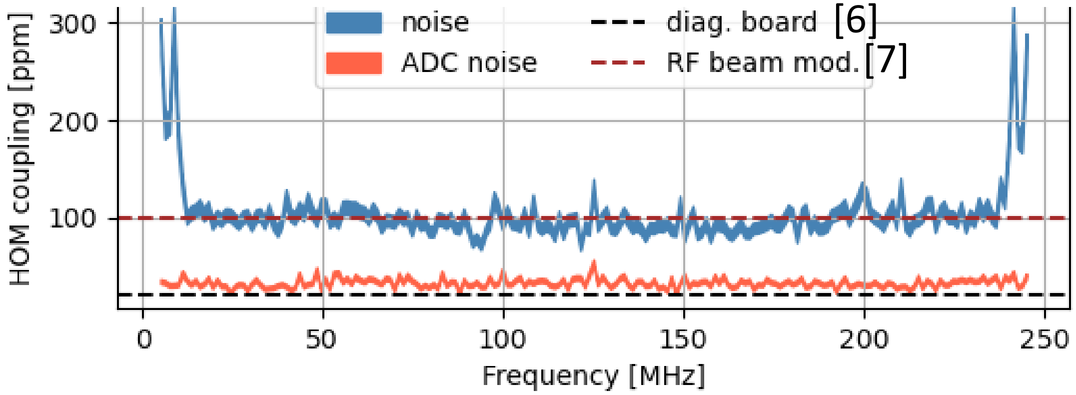

Mode basis changes and higher order modes

Beam in the laser mode basis $\Psi'_{0,0}(x,y) = H'_0(q_x)H'_0(q_y)$

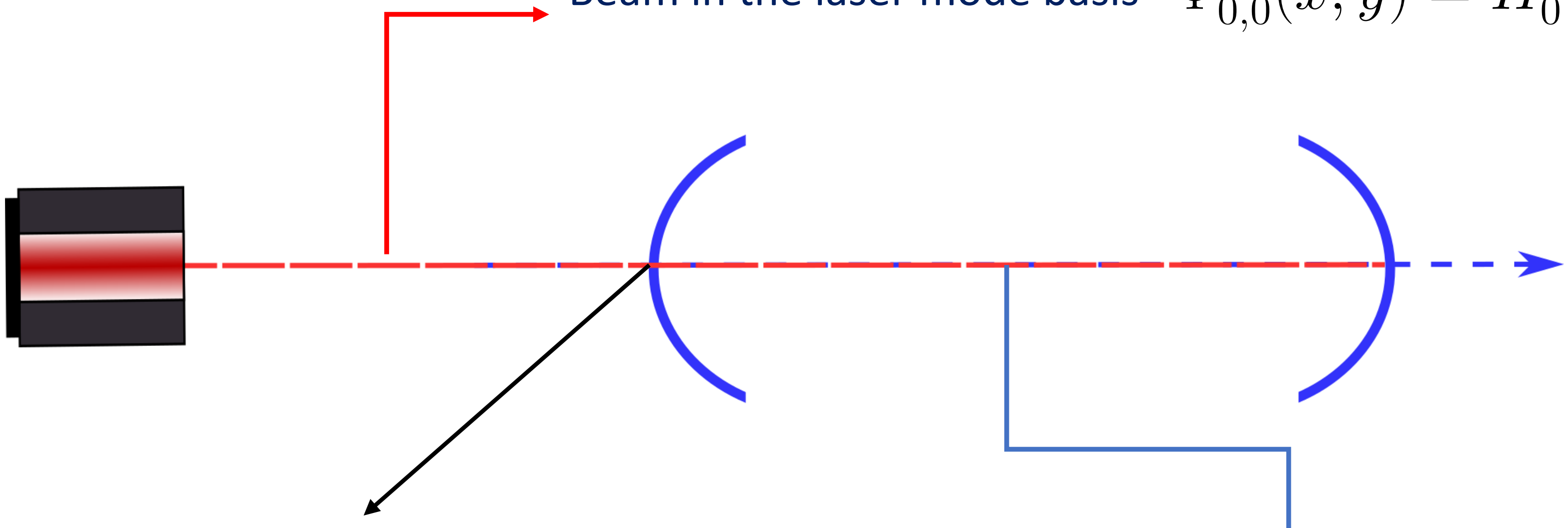

Mode basis change
(misalignment and mismatch)

$$K = \begin{pmatrix} k_{0',0} & \dots & k_{0',j} & \dots & k_{0',N} \\ \dots & \dots & \dots & \dots & \dots \\ k_{i',0'} & \dots & k_{i',j'} & \dots & k_{i',N} \\ \dots & \dots & \dots & \dots & \dots \\ k_{N',0} & \dots & k_{N',j} & \dots & k_{N',N} \end{pmatrix}$$

Beam in the cavity
mode basis

$$\Psi_{mn}(x,y) = H_m(q_x)H_n(q_y)$$

PDH + second sideband modulation

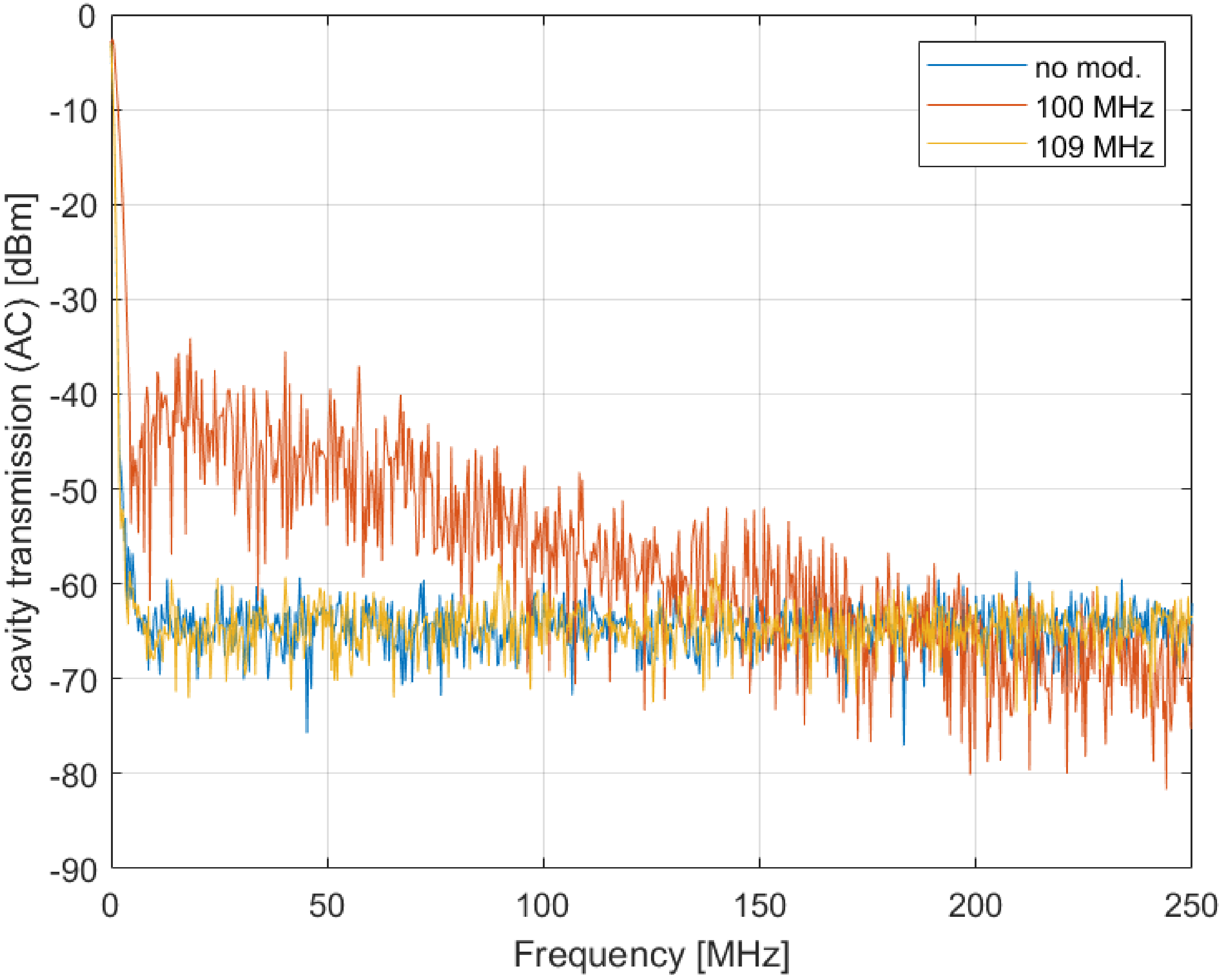

- PDH frequency = 50 MHz.
- The PDH lock is unaffected except for scanning frequencies at the PDH frequency times n (natural number).